Microwave Review
December 2024, Vol. 30, No. 2, pp. 152-158
DOI: 10.18485/mtts_mr.2024.30.2.18

Optimized Multi-target Localization in UHF RFID Systems: Leveraging Wavelet Neural Network and Non-Linear Filtering Techniques

Anand Vardhan Bhalla, Agya Mishra

Abstract – **The escalating utilization of mobile devices and the Internet of Things (IoT) has spurred extensive research in Radio Frequency Identification (RFID) to develop advanced indoor localization algorithms. However, conventional RFID-based indoor localization algorithms often fall short in delivering optimal performance. This limitation arises from the challenges associated with setting up a substantial number of antennas and the relatively small dimensions of the signal feature vector.In light of these challenges, this article presents a novel approach that addresses these issues by introducing a Wavelet Neural Network (WNN) and Extended Kalman Filter (EKF) based indoor localization and tracking algorithm. The proposed algorithm strategically employs received signal strength indicator (RSSI) and phase as feature input vectors, aiming to enhance accuracy. Our proposed technique has the advantage of accurately localising multiple tags in closed spaces, despite several constraints such as coupling effect, Non-Line of Sight (NLOS) propagation, multi-path propagation, and lack of pre-deployed reference tags. Experimental results show a substantial improvement in Localization Error, Root Mean Square Error (RMSE), Mean Absolute Error (MAE), and Localization Error Offset (LEO).**

Keywords – **RFID, WNN, Artificial Intelligence (AI), Ultra High Frequency (UHF), Received Signal Strength Indication (RSSI), EKF.**

I. INTRODUCTION

The escalating prevalence of mobile systems and the growing prevalence of indoor activities underscore the critical significance of indoor localization within the domains of wireless sensor networks and pervasive computing. UHF RFID technology stands out as a focal point due to its economic viability, easy installation, minimal power consumption, uncomplicated deployment, low latency, high precision, extensive range, and adaptability in challenging environmental conditions [1,2]. In contrast, the Global Positioning System (GPS) proves impractical for indoor applications owing to challenges associated with multipath reflection and pronounced attenuation of satellite signals due to impediments posed by surrounding structures and complex indoor environments [3,4].

Various methods have been used to address indoor localization and tracking issues, including infrared, ultrasonic, WLAN, Bluetooth, and RFID[5,6]. Among them, RFID is the most preferred technology due to its benefits. However, in complex indoor environments, RFID suffers from multipath and NLOS propagation, which severely affects the quality of measured radio signals[7,8]. Several solutions have been proposed to mitigate these adverse effects, such as time of arrival (TOA), time difference of arrival (TDOA), phase of arrival (POA), phase difference of arrival (PDOA), received signal strength indicator (RSSI), etc[3,7,9].

Presently, operational RFID tag positioning heavily relies on Received Signal Strength Indicator (RSSI). But because indoor environments are complex, it can be difficult to determine the specific distance based on signal strength between the RFID reader and the tag position, which can result in large inaccuracies and compromise the accuracy of tag localization [10]. Additionally, trilateral methods often entail complex mathematical calculations, making them impractical for widespread use. In scene analysis, location parameters are computed to construct an information plan for a specific localization scenario, followed by determining the point most likely to exhibit the feature characteristic of the desired located point [7,11,12].

Machine learning approaches, such as neural networks (NN), support vector machines, and K-nearest neighbours, have been introduced recently to improve indoor localization [13]. However, scene analysis demands an extensive reference tag signal strength dataset for increased accuracy, making it a labour-intensive and time-consuming process. Furthermore, deploying a substantial number of antennas in the localization field proves costly and impractical, resulting in a diminished signal feature vector dimension that adversely affects positioning accuracy [7,14].

Recent literature underscores the heightened sensitivity of phase information in signals to distance, presenting an opportunity to improve accuracy in indoor localization [3,5]. Nevertheless, phase cannot be directly considered a feature due to its impact on training effectiveness. Precise phase information collection and database enhancement for the training model necessitate the use of appropriate aerial placement structures [5].

To surmount these challenges, this paper introduces a Wavelet Neural Network (WNN) and Extended Kalman Filter (EKF) based indoor localization and tracking algorithm. This algorithm utilizes both RSSI and phase as feature input vectors, demonstrating notable enhancements of67%, 87.5%, 62%, and 27% in Localization Error, RMSE, MAE, and LEO respectively. The proposed method holds promise for achieving accurate indoor localization and tracking in

Article history: Received May 13,2024; Accepted May 31, 2024

Anand Vardhan Bhalla and Agya Mishra are with the Department of Electronics & Telecommunication, Jabalpur Engineering College Jabalpur, Madhya Pradesh, Pin-482011, India, E-mail: anand.bhalla1983@gmail.com, agyamishra@gmail.com

complex indoor environments, offering significant advantages for applications such as asset tracking, surveillance, and location-based services.

In this work, the input feature vector combines RSSI and phase information, achieving improved dimensionality through the incorporation of hidden layers in the NN. The WNN and EKF-based indoor localization algorithm leverage an orthogonal wavelet function as an activation function in the hidden layer. The use of orthogonal wavelet functions presents an advantage in time-frequency resolution, particularly when dealing with signals exhibiting abrupt changes [1,15,16]. Additionally, the network can adjust the resolution scale dynamically to maintain approximation accuracy. The orthogonality of the function bases facilitates seamless addition or deletion of network nodes during training, minimizing disruption to pre-existing network weights and reducing learning time [1,17,18]. The uncertainties, irregular sampling, non-linearity, and multivariate nature inherent in RFID localization and tracking measurements pose challenges that traditional algorithms are ill-equipped to address [19,20]. To address these flaws in the RFID measurement model, a non-linear filter EKF is employed.

The remaining portions are categorised as: Section II contains Measurement Model, Section III, Proposed Algorithm Section IV, Experimental setup and results, Finally, Section V conclusion.

II. MEASUREMENT MODELLING

i) UHF RFID RSSI: RSSI is measured by RSSI ranging model. The signal received from the antenna is linked to distance logarithmically. Because of severe restrictions and interference, inside settings are more complex than outdoor ones, and as a result, signal strength decreases as indoor environment distance increases [7,21]. Using a logarithmic model of path loss, the correlation between signal intensity and the distance (d) between the RFID tag and antenna is illustrated as

$$X_L(d) = X_L(d_0) + 10q\log\left({}^{d}/_{d_0}\right) + X_\sigma. \quad (1)$$

In this equation, d_o represent the reference distance, $X_L(d)$ describes the free space path loss and The symbol q stands for a path loss exponent. X_σ is a random variable with a variance of σ^2 and a standard deviation of zero. The power is expressed in dBm and the distance in meters. X_σ is introduced as the effect of shadow fading, which is result of obstacles and multipath interference. The RSSI is given by

$$\boldsymbol{X_L(d_0) = X_t - P_L(d_0)}. \quad (2)$$

$P_L(d_0)$ represents the received power which has a normal distribution, X_t denotes the transmitted power from transponder.

Let there be N (N= 1,2,3……n) number of antennas which are fused with 2D coordinated as (X_N,Y_N). Let (X_O,Y_O) be the coordinates of the object/RFID tag. Then the estimated distance $\boldsymbol{R'_{N,O}}$ between the antenna and the RFID tag calculated by

$$\boldsymbol{R'^2_{N,O} = (X_N - X_O)^2 + (Y_N - Y_O)^2}. \quad (3)$$

The error $E_{N,O}$ between the real distance $R_{N,O}$ and the estimated distance $R'_{N,O}$ is given by

$$\boldsymbol{R^2_{N,O} - R'^2_{N,O} = E^2_{N,O}}. \quad (4)$$

This is a multi-iteration method. The Mean Localization Error (MLE) for M number of iteration is given by

$$\boldsymbol{MLE = \frac{1}{M}\sum_{N=1}^{M} E^2_{N,O}}. \quad (5)$$

This work incorporates phase information, in addition to distance, in its analysis. A radio frequency (RF) signal's phase can be stated as the product of the angular frequency (ω) and the propagation time (τ). Complex demodulation provides a straightforward method to obtain the phase[1,7]. As illustrated in Figure 1, phase information can serve as a viable substitute for TOA measurements to determine distance.

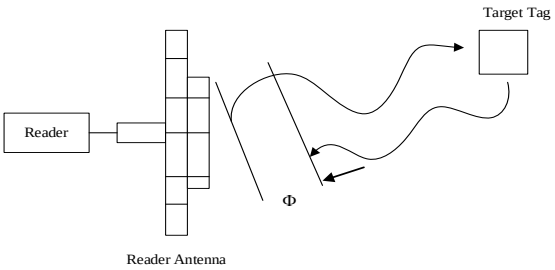

Fig. 1. Phase data used in measuring distance

As the range varies by half a wavelength, the phase undergoes a period change. The phase information is related to the Line of Sight (LoS) distance R and can be represented mathematically as:

$$\boldsymbol{\phi = \frac{-4\pi R}{\lambda} + \phi'}, \quad (6)$$

where $\boldsymbol{\lambda}$ is the working wavelength, $\boldsymbol{\phi}$ is the phase value, and $\boldsymbol{\phi'}$ is the extra phase brought on by the hardware. The phase varies monotonically over a range of half a wavelength. Nevertheless, using ultra-high frequencies results in ambiguous phase and a half wavelength that is too short for direct application. Hence, in real scenarios, it is necessary to resolve the ambiguity [5,7].

Phase-based spatial identification can be accomplished in three primary ways: Space Domain Phase Difference of Arrival (SD-PDOA), Time Domain Phase Difference of Arrival (TD-PDOA), and Frequency Domain Phase Difference of Arrival (FD-PDOA). A reliable method for preventing multipath effects is TD-PDOA. It is easy to determine the direction of movement and the point where the tag crosses the centre while employing TD-PDOA [5,7].

Moreover, the velocity profile in the direction of LoS can be calculated using TD-PDOA. In the TD-PDOA method, as shown in Figure 2, a tag circles the reader antenna at a consistent rate. If the additional phase shift and the ambient are both constant and stable, the velocity profile can be determined using the derivative of the phase difference with respect to the duration discrepancy. The following is how the radial velocity profile is expressed: $\boldsymbol{V_r = \frac{\lambda}{4\pi}\frac{(\Delta\phi - \Delta\phi')}{\Delta t}}$, (7)

where; $\boldsymbol{\phi_1 - \phi_2}$, $\boldsymbol{\Delta\phi' = \phi_1' - \phi_2'}$ and $\boldsymbol{\Delta t = t_1 - t_2}$.

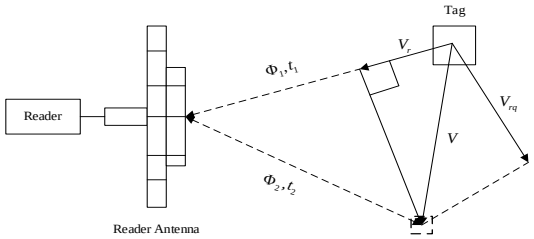

Fig. 2. TD-PDOA schematic diagram

Although TD-PDOA has the advantages of lower computation requirements and equipment costs, it is not suitable for scenarios where the tag moves at high speeds [7].
On taking angle dependent losses into consideration

$$\boldsymbol{X_{rec}(d,\phi) = X_L(d) + L_D(\phi),} \quad (8)$$

$\boldsymbol{L_D(\phi)}$is angle dependent loss and depends on $\boldsymbol{\phi}$ only. The relation between *d* and $\boldsymbol{X_{rec}(d,\phi)}$ is given by

$$\boldsymbol{d = d_0 10^{\frac{X_L(d_0)+X_\sigma+L_D(\phi)-X_{rec}(d,\phi)}{10q}}}. \quad (9)$$

RSSI in terms of $\boldsymbol{X_\sigma, \phi \; and \; L_D(\phi)}$ is

$$\boldsymbol{X_{rec}(d,\phi) = X_L(d_0) - 10qlog\left(\frac{d_e-d-\delta d}{d_0}\right),} \quad (10)$$

$\boldsymbol{d_e}$ is estimated distance and $\boldsymbol{\delta d}$ is distance error.

$$\boldsymbol{d = d_0 10^{\frac{X_L(d_0)-X_{rec}(d,\phi)}{10q}}}. \quad (11)$$

The distance error is specified by

$$\boldsymbol{\delta d = d - d_e} \quad (12)$$

ii) Wavenets: An alternative to conventional neural networks (CNN) for approximating arbitrary nonlinear functions is the WNN or Wavenet, formed by integrating the wavelet transform (WT) with the fundamental principles of NN[1,13]. Performance of the system is improved when the wavelet function takes over the role of a traditional neural network's hidden layer. The hidden layer threshold is also determined using the wavelet function. The Wavenet algorithm primarily consists of minimizing the approximation error and constructing self-built networks.

In the initial step, Wavenet conducts a detailed study on representational network architectures. The network progressively adds hidden units to efficiently cover the time-frequency area relevant to the outlined goal. Simultaneously, network parameters are updated to maintain topology and apply post-processing. In the second process, initialized network parameters undergo updates using an adaptive parametric technique based on the gradient descent algorithm to minimize approximations of instantaneous errors [22,23]. The optimization rule is selectively applied to hidden units with a square window in the time-frequency plane, encompassing the chosen point.

The suggested WNN model, as shown in Figure 3, consists of three layers, each of which performs a different function: an input layer, a hidden layer (also known as the wavelet or wavelon layer), and an output layer. Similar to neurons in traditional neural networks, the wavelon layer gets information from the input layer [17]. This layer enlarges and translates the wavelet function to create the wavelet series.

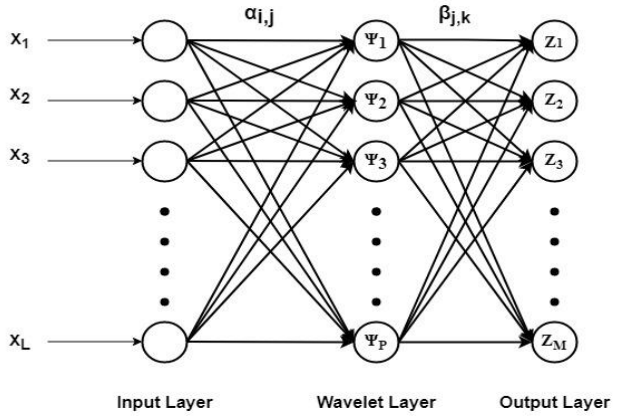

Fig3. Threelayer' WNN structure

Several types of wavelet functions can be used in WNN. In this Mexican Hat wavelet function is utilised which is defines as

$$\boldsymbol{\Psi(x) = (1 - x^2)e^{\frac{-x^2}{2}}}, \quad (13)$$

Ψ_j for each node is derived from its mother wavelet function as

$$\boldsymbol{\Psi_j(x) = \Psi(a_0\sigma - b_0)}, \quad (14)$$

where, $\sigma = \sum_{i=1}^{L_i} \alpha_{i,j} x_i$.

The wavelet's translation and dilation factors are marked by a_0 and b_0, respectively. L_i is the number of input layer nodes, and x_i is the input variable.The connection weight between the i^{th} input layer and the j^{th} wavelon in the wavelon layer is denoted by $\alpha_{i,j}$, while the connection weight between the j^{th} wavelon in the wavelon layer and the k^{th} output variable is $\beta_{j,k}$.Output of WNN is given by

$$\boldsymbol{Z_k = \sum_{j=1}^{P} \beta_{j,k}\Psi_j(x)}, \quad (15)$$

where *k*= 1,2,3……..*M*.

iii) Extended Kalman Filter (EKF): When variables of interest are indirectly assessable amid noisy measurements, the Kalman Filter (KF), an optimal estimation algorithm, is widely employed [24]. Specifically designed for linear systems, the KF predicts parameters like position, speed, or direction in the presence of noise and data uncertainties[25]. Nonlinear systems have extensions like the EKF, Unscented Kalman Filter (UKF), with the EKF being the most popular among them [16].

Nevertheless, electromagnetic interference (EMI) creates non-Gaussian time-variant noise with a non-zero mean when the EKF is used close to electric transmission lines, necessitating the use of an alternate methodology for parameter estimation.

The KF's foundation lies in assessing the likelihood of the anticipated state hypothesis given the prior state hypothesis. This probability guides correction using data from

measurement sensors, integrating measurement and prediction against process and measurement noise [27].

In utilizing the EKF, the system's model is crucial, and two EKF models exist for nonlinear discrete time systems with linear observations. Linearization is achieved by applying the Jacobian and Extended Jacobian models to the nonlinear system[28].

In summary, the KF is a potent tool for estimating parameters amid noise and errors. The EKF, a nonlinear variant, is commonly used but requires careful consideration of specific conditions, such as EMI near electric transmission lines. Adequate modeling and linearization are vital, with various models available for different systems.

An iterative algorithm, the EKF, estimates a dynamic system without direct data. It forecasts past, present, and future states based on prior knowledge, remarkable for estimating the current state without needing full history or past data. The estimation of the state and the error covariance matrix from the previous time step are among the inputs, along with the current measurement [2][29].

iv) Evaluation Parameters: The advantages of the proposed system are verified on the basis of following parameters

Mean Localization error:This is average error in localising an object.

$$\boldsymbol{e = \frac{1}{n}\sum_{i=1}^{n}\sqrt{(x - x_i)^2 + (y - y_i)^2}.} \quad (16)$$

Root Mean Square Error: This is the square root of the standard deviation, or mean square, between the predicted and actual locations.

$$\boldsymbol{RSME = \sqrt{\frac{\sum_{i=1}^{n}(x-x_i)^2}{n}}.} \quad (17)$$

*Mean Absolute Error:*It calculates the average error size over a group of projections without taking into account their directions.

$$\boldsymbol{MAE = \frac{\sum_{i=1}^{n}\|x-x_i\|}{n}.} \quad (18)$$

Localization Error Outage: LEO specifies probability of error exceeding some threshold (TH).

$$\boldsymbol{LEO = P(\|x - x_i\| > T_H),} \quad (19)$$

whereas (x,y) represents the target tag's expected coordinates, (x_i, y_i) represents the target tag's actual location.

III. Proposed Algorithm

Algorithm flow:

1. RSSI Data Acquisition: Collecting RSSI signals from all RFID tags aids in identifying their locations under specific antennas.
2. Training Data: The implemented system undergoes training using RSSI values received at antennas.
3. Sample Generation: Generating samples at 0.05-second intervals from received data, inputting them into a three-layer WNN enhances accuracy. To create a non-linear mapping between RSSI and separation, the WNN uses the separation matrices of reference tags and their RSSI values as training data. With the help of this mapping, it is possible to forecast the distance between the goal tag and antennas using RSSI, which is measured by the antenna. The objective tag's position is computed by building a variable equation set, which is then converted into an optimization problem that is solved iteratively. WNN output serves as input to EKF.
4. Localization and Error Estimation: Locating all RFID tags and calculating localization errors.
5. Output Generation: WNN processes input samples, generating the desired RFID track.
6. Parameter Calculation: Calculating and comparing localization error, RMSE, MAE, and LEO with traditional systems. Predicting the target tag-antenna separation aligns with the mapping relation constructed from the target tag's features. Employing WNN iterations intensifies location accuracy. Figure 4 illustrates the proposed system's flowchart.

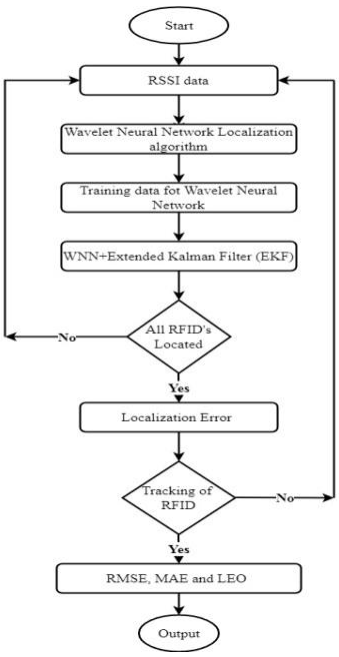

Fig. 4. Proposed system flowchart.

IV. Experimental Setup and Results

In the proposed work, four RFID antennas are strategically placed at the corners of a 50x50 meter area. Ten RFID tags are utilized for efficient localization. Figure 5 illustrate the antenna configuration and localization setup. Assuming a direction loss attenuation component of 2.4, the antennas are positioned at (0, 0), (0, 50), (50, 0), and (50, 50) for comprehensive coverage of the designated area.

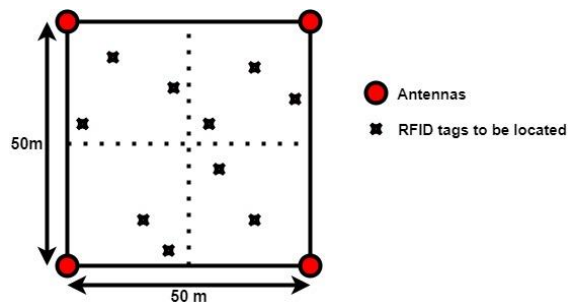

Fig5. Environmental setup.

Tables 1 and 2 present equipment specifications and corresponding RSSI values for multi-target localization. A randomly chosen object from localized objects undergoes tracking. The figure 6 illustrates RFID tag/object localization of 10 tags using the proposed system. Signal strength decreases as the object moves away from the RFID antenna, causing a shadowing effect due to the indoor environment's complexity and obstructions.

TABLE 1
EQUIPMENT SPECIFICATIONS

RFID Tag	RSI 611	
Antenna	Gain	8dB
	Polarization	LHCP
	Frequency	851.625 MHz

TABLE 2.
RSSI VALUES FROM FOUR ANTENNAS IN dBm

Antenna/RFID tag	1	2	3	4	5	6	7	8	9	10
Antenna 1	99.32	93.79	15.62	6.95	80.12	36.87	2.54	98.48	18.51	96.32
Antenna 2	11.59	34.67	98.77	99.75	59.83	92.95	99.96	17.55	98.27	26.87
Antenna 3	55.11	82.75	21.78	10.04	93.34	59.57	2.03	68.68	48.79	75.64
Antenna 4	84.44	56.13	97.59	99.49	35.86	80.31	99.97	72.68	87.28	65.40

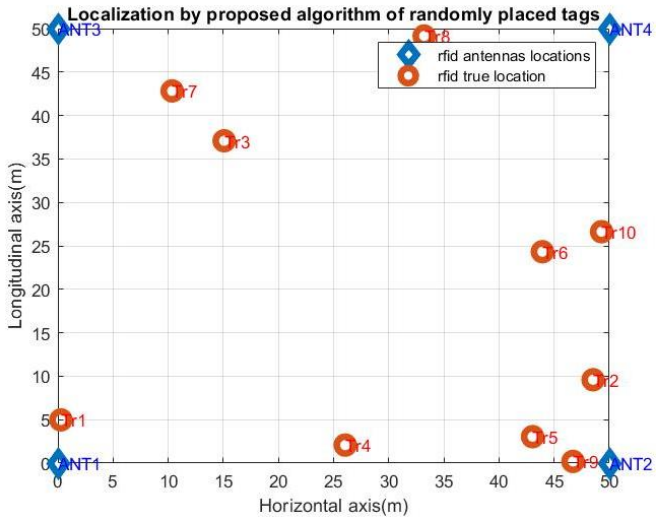

Fig. 6. Localization of RFID tags/objects

The localization error of the proposed algorithm is found to be 0.03 meters, which is far less than the BPSVR algorithm[5] in which it is 0.09 meters. Accuracy of the proposed system is enhanced by 63%.The graph representing localization error is shown in figure 7 below. After localization one of the RFID tags/objects can be tracked randomly. Trajectory and tracking of fifth RFID tag/object is shown in figures 8. The graphical representation of evaluation parameters RMSE, MAE and LEO for all 10 tags is shown in figure 9. For a comparison between the traditional algorithm and the proposed algorithm, a tabular comparison of evaluation parameters is given in Table 3.

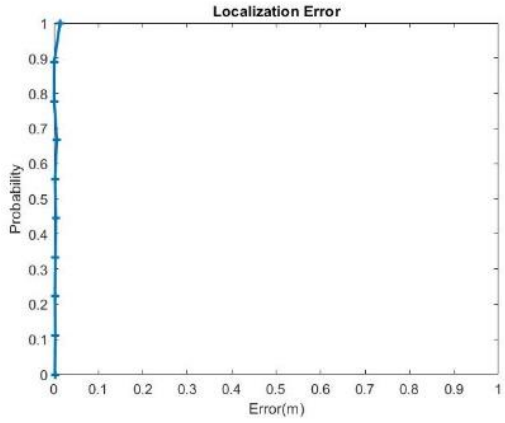

Fig. 7. Localization error by proposed algorithm

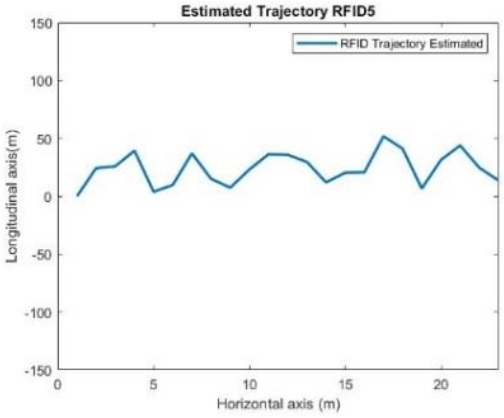

(a)

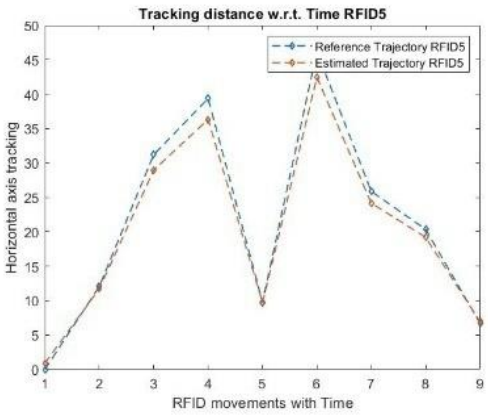

(b)

Fig. 8. (a) Estimated trajectory, (b) Tracking of fifth RFIDtag/Object

Table 3 reports numerical outcomes, indicating a substantial reduction in localization error (9cm to 3cm), RMSE (24cm to 3cm), MAE (21cm to 8cm), and improved LEO (0.4 to 0.29). The system's accuracy significantly improves. The combined use of WNN and EKF effectively identifies and tracks objects. WNN's learning and feature extraction, coupled with EKF's real-time problem handling, make the model highly efficient. WNN captures nonlinearities at different scales, while EKF algorithm accurately predicts past, present, and future states, offering a promising solution for object tracking and identification.

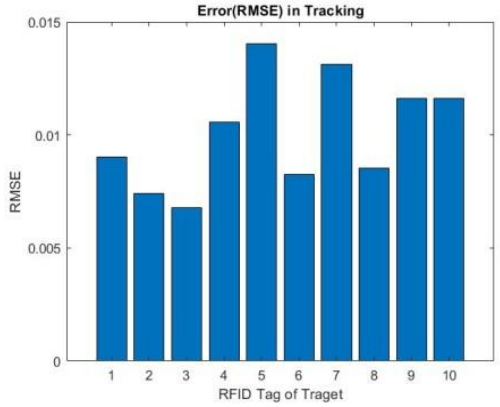

(a)

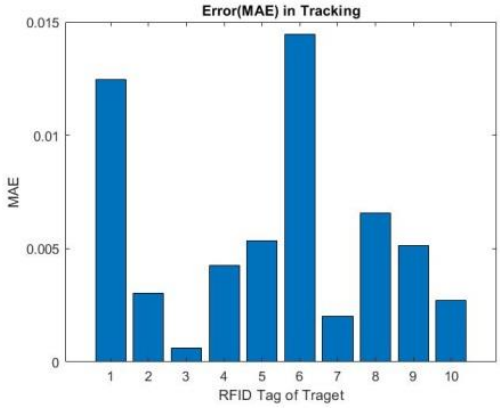

(b)

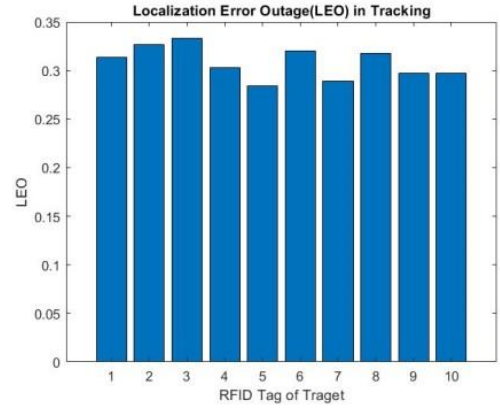

(c)

Fig. 9. Evaluation parameters for 10 target tags: (a) RMSE, (b) MAE, (c) LEO

TABLE 3.
COMPARISON OF PARAMETERS

Parameter	Traditional method	Proposed method	Improvement percentage
Localization error	0.09m	0.03m	67%
RMSE	0.24m	0.03m	87.5%
MAE	0.21m	0.08m	62%
LEO	0.4	0.29	27.5%

V. CONCLUSIONS

The proposed indoor multi-target localization and tracking method, combining WNN and EKF, outperforms conventional approaches by leveraging their respective strengths. WNN excels in capturing time and frequency domain characteristics, handling non-linear and non-stationary data, while EKF precisely tracks target objects in real-time. The fusion enhances accuracy and robustness. Using RSSI and phase as feature input vectors provides additional benefits, improving signal strength and angle of arrival estimation for precise localization. Experimental results show substantial improvements in key metrics—67%, 87.5%, 62%, and 27.5% for Localization error, RMSE, MAE, and LEO, respectively. The synergy of WNN, EKF, RSSI, and phase elevates accuracy and robustness, with implications for industries like healthcare, retail, and manufacturing in refining indoor positioning systems.

REFERENCES

[1] T. Guo, T. Zhang, E. Lim, M. Lopez-Benitez, F. Ma, and L. Yu, "A Review of Wavelet Analysis and Its Applications: Challenges and Opportunities", *IEEE Access*, vol. 10, pp. 58869–58903, Jun. 2022, DOI: 10.1109/access.2022.3179517.

[2] J. Damade and A. Mishra, "RFID Based Application Algorithms for Communication System: A Literature Review", *Int. J. Comput. Sci. Eng*., 2017.

[3] Y. Zhao, K. Liu, Y. Ma, Z. Gao, Y. Zang and J. Teng, "Similarity Analysis-Based Indoor Localization Algorithm With Backscatter Information of Passive UHF RFID Tags," in *IEEE Sensors Journal*, vol. 17, no. 1, pp. 185-193, 1 Jan.1, 2017, DOI: 10.1109/JSEN.2016.2624314

[4] P. Devika, V. Prashanthi, G. V. Kanth, and J. Thirupathi, *RFID Based Theft Detection and Vehicle Monitoring System using Cloud*, 2019. [Online]. Available at: http://ageqnies.com/html/rfid.html

[5] L. Mo, Y. Zhu and D. Zhang, "UHF RFID Indoor Localization Algorithm Based on BP-SVR," in *IEEE Journal of Radio Frequency Identification*, vol. 6, pp. 385-393, 2022, DOI: 10.1109/JRFID.2022.3145153.

[6] X. Huang, H. Cheena, A. Thomas, and J. K. P. Tsoi, "Indoor Detection and Tracking of People Using mmWave Sensor", *J. Sensors*, vol. 2021, 2021, DOI: 10.1155/2021/6657709.

[7] C. Li, L. Mo and D. Zhang, "Review on UHF RFID Localization Methods," in *IEEE Journal of Radio Frequency Identification*, vol. 3, no. 4, pp. 205-215, Dec. 2019, DOI: 10.1109/JRFID.2019.2924346

[8] J. Pegoraro and M. Rossi, "Real-Time People Tracking and Identification From Sparse mm-Wave Radar Point-Clouds," in *IEEE Access*, vol. 9, pp. 78504-78520, 2021, DOI: 10.1109/ACCESS.2021.3083980

[9] M. S. Rohei, E. Salwana, N. B. A. K. Shah and A. S. Kakar, "Design and Testing of an Epidermal RFID Mechanism in a Smart Indoor Human Tracking System," in *IEEE Sensors Journal*, vol. 21, no. 4, pp. 5476-5486, 15 Feb.15, 2021, DOI: 10.1109/JSEN.2020.3036233

[10] H. Kong and B. Yu, "Modeling and Optimization of RFID Networks Planning Problem," *Wirel. Commun. Mob. Comput.*, vol. 2019, 2019, DOI: 10.1155/2019/2745160.

[11] L. Ma, X. Wang, M. Huang, Z. Lin, L. Tian and H. Chen, "Two-Level Master–Slave RFID Networks Planning via Hybrid

Multiobjective Artificial Bee Colony Optimizer," in *IEEE Transactions on Systems, Man, and Cybernetics: Systems*, vol. 49, no. 5, pp. 861-880, May 2019, DOI: 10.1109/TSMC.2017.2723483

[12] H. Fu et al., "Device-Free Multitarget Localization With Weighted Intersection Multidimensional Feature for Passive UHF RFID," in *IEEE Sensors Journal*, vol. 22, no. 7, pp. 7300-7310, 1 April, 2022, DOI: 10.1109/JSEN.2022.3151386.

[13] W. Sun, W. Lu, Q. Li, L. Chen, D. Mu, and X. Yuan, "WNN-LQE: Wavelet-Neural-Network-Based Link Quality Estimation for Smart Grid WSNs," *IEEE Access*, vol. 5, pp. 12788–12797, 2017, DOI: 10.1109/ACCESS.2017.2723360.

[14] A. R. Chatzistefanou, G. Sergiadis and A. G. Dimitriou, "Tag Localization by Handheld UHF RFID Reader With Optical and RFID Landmarks," in *IEEE Journal of Radio Frequency Identification*, vol. 7, pp. 330-340, 2023, DOI: 10.1109/JRFID.2023.3238822.

[15] N. Soni and D. A. Mishra, "The Intuitive Supervision Model (ISM) using Convolution Neural Networks (CNN) and Unscented Kalman Filters (UKF)," *International Journal of Recent Technology and Engineering (IJRTE)*, vol. 10, no. 5, pp. 117–124, Jan. 2022, DOI: 10.35940/ijrte.E6782.0110522.

[16] S. Heo, J. Cha, and C. G. Park, "EKF-Based Visual Inertial Navigation Using Sliding Window Nonlinear Optimization", *IEEE Transactions on Intelligent Transportation Systems*, vol. 20, no. 7, pp. 2470–2479, 2019, DOI: 10.1109/TITS.2018.2866637.

[17] W. Sun, W. Lu, Q. Li, L. Chen, D. Mu, and X. Yuan, "WNN-LQE: Wavelet-Neural-Network-Based Link Quality Estimation for Smart Grid WSNs," *IEEE Access*, vol. 5, pp. 12788–12797, Jul. 2017, DOI: 10.1109/ACCESS.2017.2723360.

[18] O. F. Lutfy, "Wavelet Neural Network Model Reference Adaptive Control Trained by a Modified Artificial Immune Algorithm to Control Nonlinear Systems," *Arabian Journal for Science and Engineering*, vol. 39, no. 6, pp. 4737–4751, 2014, DOI: 10.1007/s13369-014-1088-5.

[19] F. Hu and G. Wu, "Distributed Error Correction of EKF Algorithm in Multi-Sensor Fusion Localization Model," in *IEEE Access*, vol. 8, pp. 93211-93218, 2020, DOI: 10.1109/ACCESS.2020.2995170.

[20] C. Tian, Y. Ma and B. Wang, "Cooperative Localization for Passive RFID Backscatter Networks and Theoretical Analysis of Performance Limit," in *IEEE Transactions on Wireless Communications*, vol. 22, no. 2, pp. 1388-1402, Feb. 2023, DOI: 10.1109/TWC.2022.3204679..

[21] A. Yassin et al., "Recent Advances in Indoor Localization: A Survey on Theoretical Approaches and Applications," *IEEE Commun. Surv. Tutorials*, vol. 19, no. 2, pp. 1327–1346, 2017, DOI: 10.1109/COMST.2016.2632427.

[22] O. F. Lutfy, "Wavelet Neural Network Model Reference Adaptive Control Trained by a Modified Artificial Immune Algorithm to Control Nonlinear Systems," *Arabian Journal for Science and Engineering*, vol. 39, no. 6, pp. 4737–4751, 2014, DOI: 10.1007/s13369-014-1088-5.

[23] B. Krishna, Y. R. Satyaji Rao, and P. C. Nayak, "Wavelet Neural Network Model for River Flow Time Series", *Proc. Inst. Civ. Eng. Water Management*, vol. 165, no. 8, pp. 425–439, Sep. 2012, DOI: 10.1680/wama.10.00092.

[24] F. Liu, P. Zhao, and Z. Wang, "EKF-Based Beam Tracking for mmWave MIMO Systems," *IEEE Communication. Letter*, vol. 23, no. 12, pp. 2390–2393, 2019, DOI: 10.1109/LCOMM.2019.2940660.

[25] F. Gustafsson and G. Hendeby, "Some Relations Between Extended and Unscented Kalman Filters," *IEEE Trans. Signal Process.*, vol. 60, no. 2, pp. 545–555, 2012, DOI: 10.1109/TSP.2011.2172431.

[26] X. -b. Jin, Y. Shi and C. -X. Nie, "Tracking for indoor RFID System with UKF and EKF," *2015 International Conference on Estimation, Detection and Information Fusion (ICEDIF)*, Harbin, China, 2015, pp. 146-151, DOI: 10.1109/ICEDIF.2015.7280179

[27] X. B. Jin, C. Dou, T. L. Su, X. F. Lian, and Y. Shi, "Parallel Irregular Fusion Estimation Based on Nonlinear Filter for Indoor RFID Tracking System," *Int. J. Distrib. Sens. Networks*, vol. 2016, 2016, DOI: 10.1155/2016/1472930.

[28] K. Shu, J. Yi, X. Wan, and F. Cheng, "A Hybrid Tracking Algorithm for Multistatic Passive Radar", *IEEE Syst. J.*, vol. 15, no. 2, pp. 2024–2034, 2021, DOI: 10.1109/JSYST.2020.2994009.

[29] A. Motroni, G. Cecchi, A. Ria and P. Nepa, "Passive UHF-RFID Technology: Integrated Communication, Localization and Sensing," in *IEEE Journal of Radio Frequency Identification*, vol. 7, pp. 564-572, 2023, DOI: 10.1109/JRFID.2023.3301093.